



Photoligation of self-assembled DNA constructs containing anthracene-functionalized 2'-amino-LNA monomers

Karol Pasternak^{a,†}, Anna Pasternak^{a,†}, Pankaj Gupta^{a,†}, Rakesh N. Veedu^{a,b,†}, Jesper Wengel^{a,*}

^aNucleic Acid Center, Department of Physics and Chemistry, University of Southern Denmark, Campusvej 55, 5230 Odense M, Denmark

^bSchool of Chemistry and Molecular Biosciences, The University of Queensland, St Lucia, Brisbane, Queensland 4072, Australia

ARTICLE INFO

Article history:

Received 7 July 2011

Revised 13 October 2011

Accepted 17 October 2011

Available online 20 October 2011

Keywords:

Amino-LNA

Anthracene

Photoligation

DNA cross-linking

ABSTRACT

Efficient synthesis of a novel anthracene-functionalized 2'-amino-LNA phosphoramidite derivative is described together with its incorporation into oligodeoxynucleotides. Two DNA strands with the novel 2'-*N*-anthracenylmethyl-2'-amino-LNA monomers can be effectively cross-linked by photoligation at 366 nm in various types of DNA constructs. Successful application of three differently functionalized 2'-amino-LNA monomers in self-assembled higher ordered structures for simultaneous cross-linking and monitoring of assembly formation is furthermore demonstrated.

© 2011 Elsevier Ltd. All rights reserved.

1. Introduction

Chemical ligation and photodimerization reactions have been implemented within synthetic chemistry, biochemistry, biomedicine, and nanotechnology.^{1–10} Accordingly, there are numerous reports concerning both chemical ligation^{3,7,8,11–14} and photoligation of nucleic acid constructs.^{15–21} Photoligation can be considered the more promising of these two non-enzymatic reactions for covalent linking of nucleic acid strands as it does not require any reagents except for the nucleic acid strands involved. Moreover, the reaction progress can be straightforwardly controlled by the duration of sample irradiation and the wavelength applied.^{3,15} As nucleic acids can be damaged by UV-B light (280–315 nm)²² it is important for potential *in vivo* applications to identify suitable photo-reactive groups which are able to form photoadducts at a wavelength safe for human cells. One such group of compounds that are photoactive above 300 nm are 9-substituted anthracene derivatives. Anthracene has been applied as an intercalator and fluorophore in nucleic acid contexts^{23,24} and is known to form photodimers after exposure to light of a wavelength of 366 nm.¹⁵

There are only few reports describing formation of covalent bonds between nucleic acid strands via anthracene photo-dimer formation,^{15,16,18} and photoligation between anthracene rings has mostly involved derivatives attached via linkers to oligonucleotide 5'- and 3'-ends. We decided to combine the photochemical properties of 9-substituted anthracene derivatives with the duplex-stabilizing and

conjugating properties of 2'-amino-LNA monomers^{25,26} to introduce covalent junctions either in the middle or at terminal positions of complementary oligonucleotides. Notably, the 2'-amino group of 2'-amino-LNA monomers gives the opportunity of introducing additional functional groups which has resulted in numerous novel oligonucleotide derivatives with various interesting properties and applications.^{26–32} Herein we report efficient synthesis of a novel 2'-amino-LNA monomer functionalized with an anthracen-9-ylmethyl group and the versatility of such monomers for photochemically induced cross-linking of complementary nucleic acid strands.

2. Results and discussion

2.1. Chemical synthesis of anthracene-functionalized 2'-amino-LNA phosphoramidite **3**

5'-*O*-(4,4'-Dimethoxytrityl)-protected 2'-amino-LNA nucleoside **1** was prepared according to previously described procedures.³³ Reductive amination of derivative **1** with 9-anthraldehyde in the presence of sodium triacetoxyborohydride³⁴ gave nucleoside **2** in 76% yield. Subsequent standard phosphitylation using 2-cyanoethyl-*N,N,N',N'*-tetraiso-propylphosphordiamidite furnished in 69% yield the anthracene-functionalized 2'-amino-LNA phosphoramidite **3** (Scheme 1) which was used on an automated DNA synthesizer to prepare oligonucleotides containing monomer **T*** (Table 1; Scheme 2; See Section 4 for details).

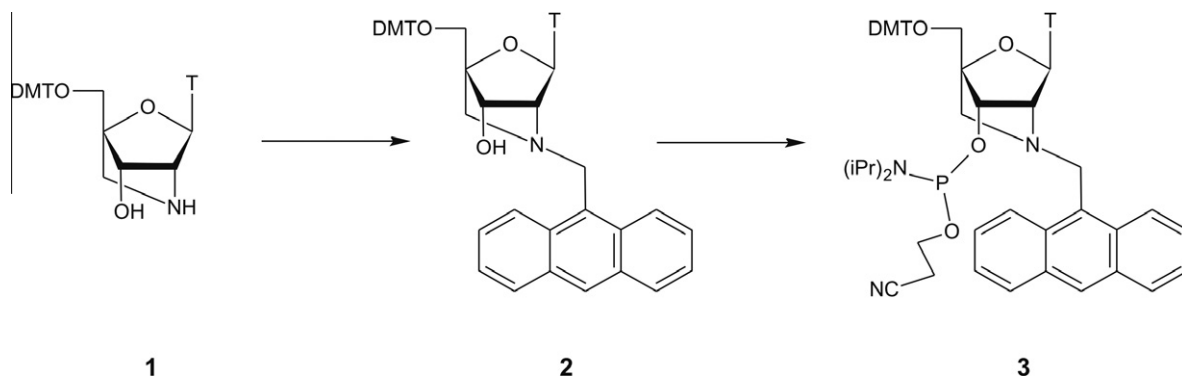
2.2. Photoligation studies

The sequences of the oligonucleotide substrates used in photoligation reactions and the expected constructs formed upon

* Corresponding author. Tel: +45 6550 2510; fax: +45 6550 4385.

E-mail address: jwe@ifk.sdu.dk (J. Wengel).

† Tel.: +45 6550 2510; fax: +45 6617 8760.



Scheme 1. Synthesis of 9-methylanthracene 2'-amino-LNA O3'-phosphoramidite derivative **3**.

Table 1
Names and sequences of oligonucleotides used in photoligation studies containing methylanthracene 2'-amino-LNA (**T***), and schematic structures of the DNA constructs studied

Oligonucleotide name	Sequence (5'→3')	Construct
ON1	CGTTTATATACAG	
ON2	T* AAACG	
ON3	CGTGAT T*	
ON4	CGTTAATATACAG	
ON5	GCAT T* ATCAC	
ON6	GTGAT T* ATGC	
ON7	GCAT T* CAC	
ON8	CTGCAACGCAACGCAACGTC	
ON9	T* GCAG	
ON10	T* GCG T*	
ON11	GACG T*	
ON12	T* CCGAAAAGCGGAACCG T*	

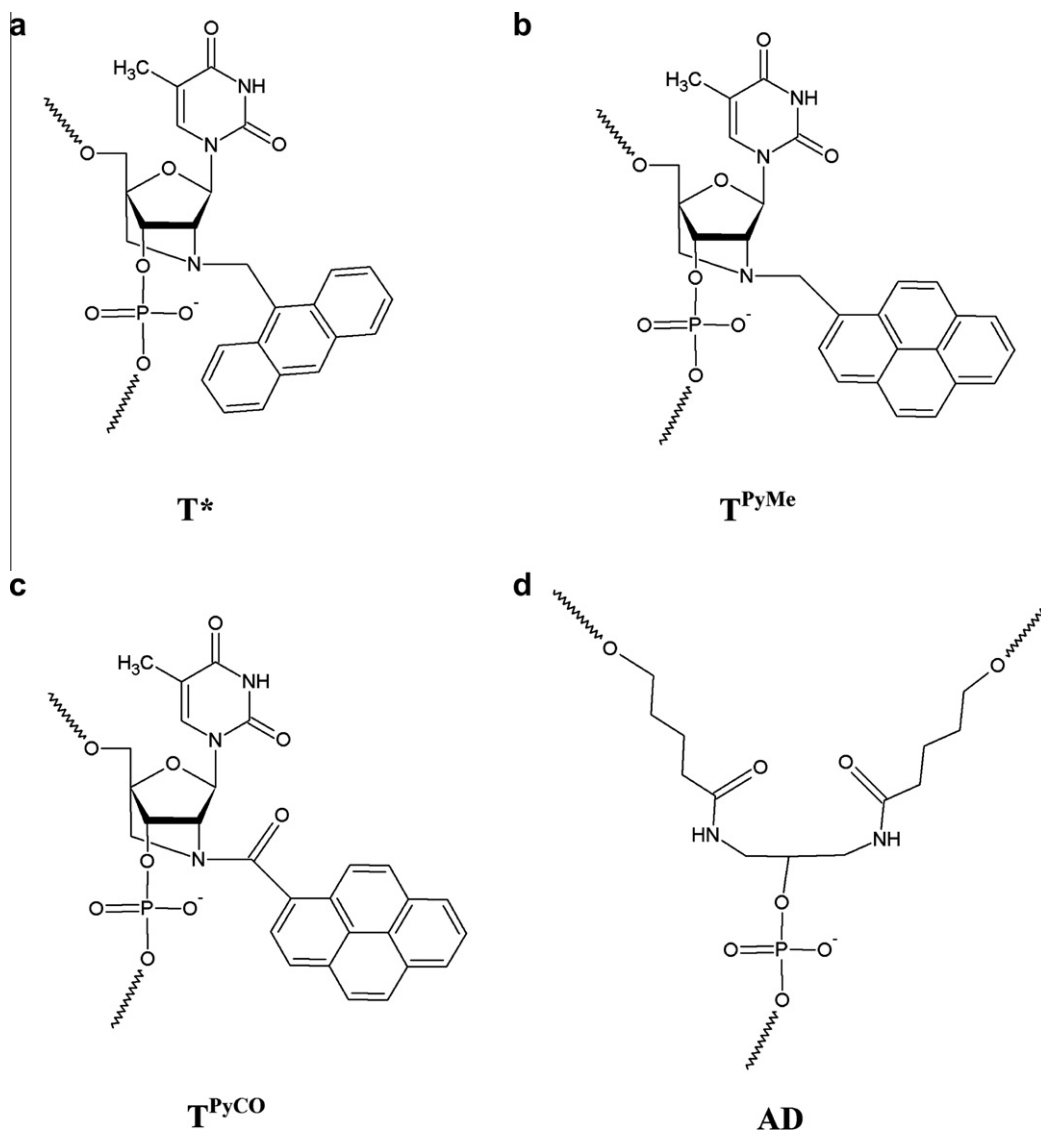
hybridization are shown in Table 1. **ON2** and **ON3** contain monomer **T*** at the 5'- and 3'-end, respectively, and are designed to bind **ON1** or **ON4**. Hybridization between these oligonucleotides results in the formation of three-stranded constructs **A** and **B** with a discontinuity in the central region. The monomers **T*** of constructs **A** and **B** were positioned to evaluate the ability to link between the two anthracene-functionalized monomers in two oligonucleotides hybridizing with a one nucleotide gap (construct **A**) or juxtapositioned (construct **B**) on a template oligonucleotide. The second group of constructs **C** and **D** were designed to study cross-linking between two oligonucleotides together forming a duplex having one **T*** monomer in each strand at internal positions. From our earlier results on the formation of interstrand contacts between pyrene units attached to 2'-amino-LNA monomers²⁹ we anticipated suitable orientation of the anthracene moieties of monomers **T*** in constructs **C** and **D** for photochemical ligation and thus interstrand cross linking. Additional constructs studied are **E** formed by five oligonucleotides, and **F** formed by the self-complementary **ON12**.

To study the progress of the photochemical ligation reactions, that is, anthracene photodimer formation, we have followed the decrease of band intensities originating from the anthracene moi-

eties (at 325–400 nm).³⁵ Formation of the expected products was also tested using ion exchange HPLC and by thermodynamic stability studies. Reversibility of photoligation was tested by heating the products at 90 °C for 4 and 16 h.

Irradiation of construct **A** at 366 nm for 5 min resulted in formation of a minor amount of photoadduct. As expected the efficiency of photoligation increased over time and after 60 min almost full conversion was reached (Fig. 1a). In case of construct **B** with two juxtapositioned anthracene-functionalized 2'-amino-LNA monomers, the formation of a photoadduct was likewise observed. The reaction progress, as evaluated by UV-vis spectroscopy in the 325–400 nm region, was similar to that observed for construct **A**, although a slightly faster photoligation reaction for construct **B** was indicated (Fig. 1b). This difference indicates the importance of preorganizing the anthracene moieties in close proximity for efficient photodimerization. Formation of the photoadducts was also confirmed by HPLC chromatograms (Supplementary data Fig. 4).

Constructs **C** and **D** also formed photoadducts. The changes in band intensities in the 325–400 nm region of the UV-vis spectra indicated that the progress of the photoligation was slightly faster for construct **C** than for **D** (Fig. 1c and d), although in both cases the



Scheme 2. Chemical structures of 2'-N-amino-LNA monomers (a-c) and asymmetric doubler (d).

reactions reached full completion after irradiation for 60 min. The analysis of ion exchange HPLC chromatograms of constructs **C** and **D** after photoligation revealed formation of two main products instead of one (Supplementary data Fig. 5), probably due to the fact that 9-substituted anthracene derivatives can photodimerize according to 'head-to-tail' or 'head-to-head' geometries.³⁶ We next proceeded to testing photoligation of the higher-ordered self-assembled DNA constructs **E** and **F**. In both cases UV spectra confirmed successful formation of photodimers (Fig. 1e and f), and in case of construct **F** its formation was confirmed also by MALDI-MS (See Supplementary data).

2.3. Thermodynamics

Although many anthracene-formed photodimers are thermally unstable³⁷ we found photoadducts formed from constructs **A–D** to be thermally stable. We incubated photoligation products at 90 °C in the buffer solution used during irradiation, but no indications of reversibility in photodimer formation, even after 16 h, was indicated (Supplementary data Fig. 6). We therefore decided to calculate thermodynamic parameters for those photoadducts.

The main objective of the thermodynamic analysis was to show differences in thermodynamic stability of modified constructs before and after irradiation. Analyses of the corresponding unmodified DNA counterparts of constructs **A**, **B**, **C** and **D** were made as reference for the remaining data. Unexpectedly, the melting profiles of non-ligated constructs **A** and **B**, each composed of three strands, were characterized by a single transition. Presumably strong inter-strand stacking interactions involving the anthracene moieties induce the two short strands to melt cooperatively. Thermodynamic studies of DNA complexes before and after irradiation at 366 nm revealed decrease in thermodynamic stability of photoligated products (Table 2). Destabilization of both structures **A** and **B** after formation of anthracene photoadducts might be caused by generation of local distortions in the structure induced by the novel covalent linkage or loss of aromatic character of the anthracene rings after photoligation, what causes loss of stacking interactions between those systems. Photodimerization of duplexes **C** and **D** caused stronger decrease of thermodynamic stability (Table 2), what indicates a more prominent influence of the photoproduct when placed centrally in constructs, presumably due not only to the loss of stacking interactions between anthracene rings but most probably also to additional structural perturbations.

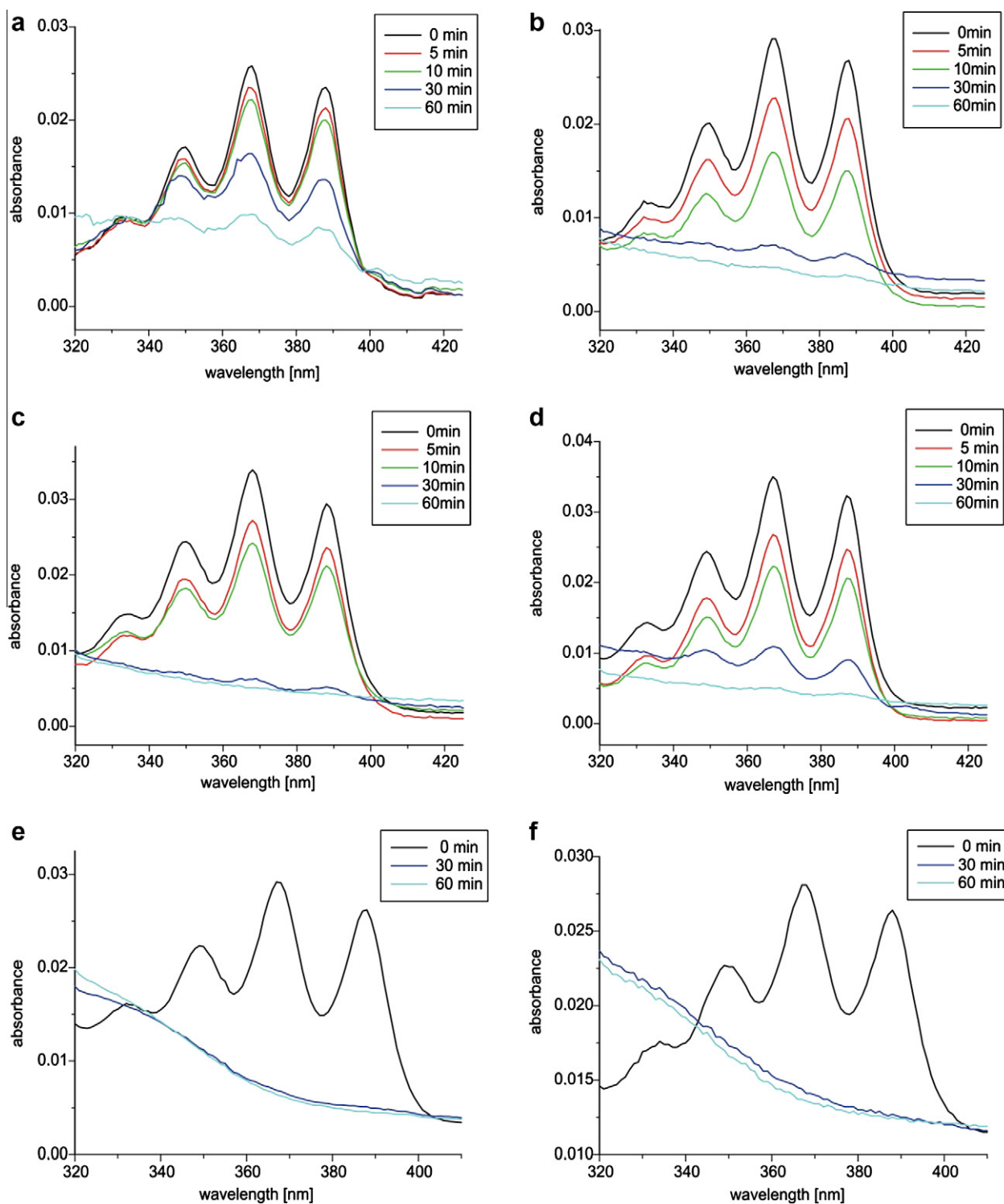


Figure 1. UV spectra of DNA constructs **A** (a), **B** (b), **C** (c), **D** (d), **E** (e) and **F** (f). Time of exposure to 366 nm UV light: 0 min–black, 5 min–red, 10 min–green, 30 min–blue, 60 min–cyan.

2.4. Formation and analysis of anthracene-based photoadducts in the presence of different 2'-amino-LNA modified monomers

To illustrate the applicability of the novel photoligation reactions we incorporated the anthracene-functionalized 2'-amino-LNA monomers T^* into **ON14** and **ON15** (Table 3). The four branched oligonucleotides **ON13–ON16** were designed to hybridize to form the simple dendrimer-like construct **I** (Table 3). One

duplex segment of the construct contains two T^* monomers for photoligation (here duplex cross-linking), another segment two 2'-*N*-(pyren-1-ylcarbonyl)amino-LNA monomers²⁸ (T^{PyCO}) and the third two 2'-*N*-(pyren-1-ylmethyl)amino-LNA monomers²⁹ (T^{PyMe}) (see Scheme 2 for structures of monomers). As positioned in construct **I**, the T^{PyMe} and T^{PyCO} monomers should signal hybridization, and thus construct formation, by excimer-band formation and monomer fluorescence light-up, respectively.^{28,29}

Table 2
Thermodynamic parameters before and after irradiation at 366 nm of DNA helix formation with 2'-N-methylanthracene 2'-amino-LNA T monomers **T^{PyMe}** incorporated^a

DNA duplexes	Reaction time (min)	−ΔH ^b (kcal/mol)	−ΔS (eu)	−ΔG ₃₇ (kcal/mol)	T _m ^b (°C)	ΔΔG ₃₇ (kcal/mol)	ΔT _m ^b (°C)
DNA reference	—	(45.7 ± 3.5)	(123.1 ± 11.5)	(7.53 ± 0.10)	(44.0)		
5'CGTTTA-T-ATATCAGC3' 3'GCAAAAT ^{5/3} -TATAGTGC5'	0 ^b	40.9 ± 0.9	105.7 ± 3.0	8.13 ± 0.01	49.7	0	0
5'CGTTTA-T-ATATCAGC3' 3'GCAAAAT ^{5/3} -T ^{PyMe} ATAGTGC5'	60 ^c	44.1 ± 7.2	118.5 ± 23.8	7.38 ± 0.34	43.1	0.75	−6.6
DNA reference	—			<7.53	<44.0		
5'CGTTTA - ATATCAGC3' 3'GCAAAAT ^{5/3} -TATAGTGC5'	0 ^b	43.7 ± 2.7	116.0 ± 8.7	7.75 ± 0.08	45.9	0	0
5'CGTTTA - ATATCAGC3' 3'GCAAAAT ^{5/3} -T ^{PyMe} ATAGTGC5'	60 ^c	55.8 ± 2.5	157.2 ± 8.3	7.04 ± 0.06	39.9	0.71	−6.0
DNA reference	—	62.5 ± 1.6	173.8 ± 5.0	8.54 ± 0.02	47.3		
5'GCAATATCAC3' 3'CGTATAGTG5'	0 ^b	(69.1 ± 11.4)	(181.9 ± 34.1)	(12.63 ± 0.80)	(67.0)	0	0
5'GCAATATCAC3' 3'CGTAT ^{PyMe} AGTG5'	60 ^c	65.4 ± 3.2	175.8 ± 10.0	10.87 ± 0.13	59.0	1.76	−8.0
Construct D	0 ^b	60.5 ± 2.8	160.5 ± 8.5	10.74 ± 0.12	60.2	0	0
5'GCAAT ^{PyMe} CAC3' 3'CGTAT ^{PyMe} AGTG5'	60 ^c	65.8 ± 2.8	180.6 ± 8.7	9.81 ± 0.07	53.3	0.93	−6.9

^a 1 M NaCl, 0.1 mM phosphate buffer, pH 7, 10^{−4} M oligomer concentration; values in parentheses are from non-two state melts.

^b Without irradiation.

^c After irradiation for 60 min.

The previous series of experiments revealed complete photoligation after 60 min which we therefore applied here. UV-spectra upon mixing of **ON14+ON15**, **ON13+ON14+ON15** and **ON13+ON14+ON15+ON16** and subsequent irradiation at 366 nm demonstrated the ability to photodimerize the two anthracene units in all three cases (Fig. 2a–c, respectively). Next we showed that photoligation is possible regardless of system complexity. This is presented in Figure 3 as no anthracene signals are observed above 350 nm after photoligation subsequent to mixing two (**ON14+ON15**), three (**ON13+ON14+ON15**) or four (**ON13+ON14+ON15+ON16**) components of construct **I**.

Fluorescence-based detection of self-assembly of branches **ON13** and **ON16** with **ON14** was possible due to hybridization-induced changes in fluorescence spectra, that is, emergence of an excimer band in the region 450–550 nm for the **T^{PyMe}** containing duplex segment and increased pyrene monomer fluorescence signals in the region 370–410 nm for the **T^{PyCO}** containing segment, respectively.^{28,29} The fluorescence picture during sequential addition of the individual branched oligonucleotides to form construct **I** is depicted in Figure 5. The starting branched oligonucleotide **ON13** shows only low fluorescence intensity as expected (black line). After hybridization with **ON14**, the emergence of a strong excimer signal is observed which can be explained by interstrand communication between the two pyrene units of the **T^{PyMe}** monomers (red line). As expected, further addition of **ON15** does not modulate the fluorescence (green line). Addition finally of **ON16** induces a significant intensity increase in the pyrene monomer fluorescence signals according to the expectation with two **T^{PyCO}** monomers positioned as in **ON16** (dark blue line). All together, the fluorescence changes described above testify to successful self-assembly of construct **I**. Eventually, photoligation was induced by UV light irradiation for 60 min which did not significantly change the fluorescence fingerprint of the mixture (light blue line) which indicates that photoligation takes place without disrupting the self-assembled construct **I** (Fig. 4).

3. Conclusions

A novel 2'-N-amino-LNA anthracene-functionalized phosphoramidite monomer has been synthesized and successfully incorporated into oligonucleotides using automated DNA synthesis. Efficient anthracene photodimer-formation was achieved in different DNA-based constructs leading to covalent interstrand crosslinks upon irradiation at 366 nm. Photodimer formation seems to be independent of oligonucleotide sequence, and can be realized even in higher-order constructs. The results described herein open new ways of constructing and designing covalently linked higher-ordered DNA constructs.

4. Experimental section

4.1. General methods

All reagents were used as purchased. Reactions under anhydrous conditions were carried out under an atmosphere of argon or nitrogen. Solvents were of HPLC grade, of which dichloromethane and dichloroethane were dried over 4 Å molecular sieves and acetonitrile over 3 Å molecular sieves. Progress in reactions was monitored by thin-layer chromatography (TLC) on analytical Merck silica gel TLC aluminium plates (60 F254) with fluorescence indicator. For column chromatography, Merck silica gel 60 (0.040–0.063 mm) was used. After column purification, fractions containing product were combined, dried over Na₂SO₄, filtrated, and evaporated to dryness at reduced pressure. ¹H NMR spectra were

Table 3
Sequences of branched oligonucleotides and scheme of 3-way junction nanoconstruct formed. Modified monomers: 2'-N-(pyren-1-yl)methyl-2'-amino-LNA thymine ((T^{PyMe})), 2'-N-(anthracene-9-yl)methyl-2'-amino-LNA thymine ((T^{*})), 2'-N-(pyren-1-yl)carbonyl-2'-amino-LNA thymine ((T^{PyCO})), asymmetric doubler ((AD)). See Scheme 2 for structures of modified monomers

Branched oligonucleotides		
Name of oligonucleotide	Sequence	Construct
ON13	5'-CGTAT ^{PyMe} GCADTAC-3' 5'-TAC	
ON14	5'-GCAT ^{PyMe} ACGADGCTTACAT-3' 5'-GCT [*] AGC	
ON15	5'-GCT [*] AGCADTAC-3' 5'-TAC	
ON16	5'-TACADAT ^{PyCO} GT ^{PyCO} AAGC-3' 5'-TAC	

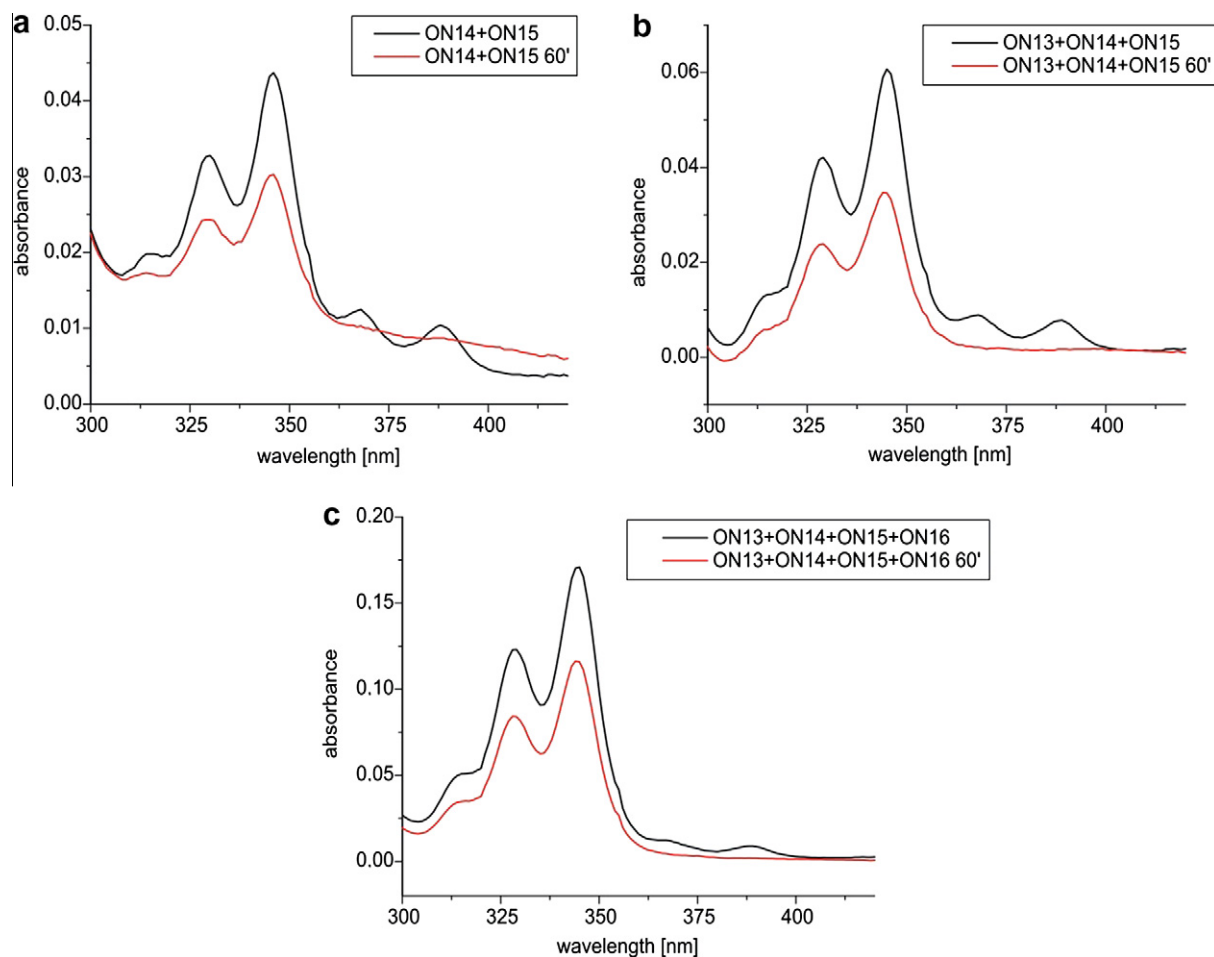


Figure 2. UV spectra comparisons before/after photoligation of systems **ON14** and **ON15** (a), **ON13**, **ON14** and **ON15** (b), and **ON13**, **ON14**, **ON15** and **ON16** (c).

recorded at 300 MHz, ¹³C NMR spectra at 75.5 MHz and ³¹P NMR spectra at 121.5 MHz. Chemical shifts are reported in ppm relative to either tetramethylsilane or the deuterated solvent (δ H: CDCl₃ 7.26 ppm; δ C: CDCl₃ 77.0 ppm) as internal standard for ¹H NMR and ¹³C NMR, and relative to 85% H₃PO₄ as an external standard for ³¹P NMR. Assignments of NMR spectra, when given are based on 2D NMR experiments (the assignments of methylene protons/

methylene carbons may be interchanged). Coupling constants (*J* values) are given in Hz. MALDI-HRMS spectra were recorded in positive ion mode on an Ion Spec Fourier transform mass spectrometer. MALDI-MS analysis of oligonucleotides was performed on a Perseptive Voyager STR (Applied Biosystems) MALDI-time-of-flight apparatus using 3-hydroxypicolinic acid as matrix in positive ion mode using delayed ion extraction.

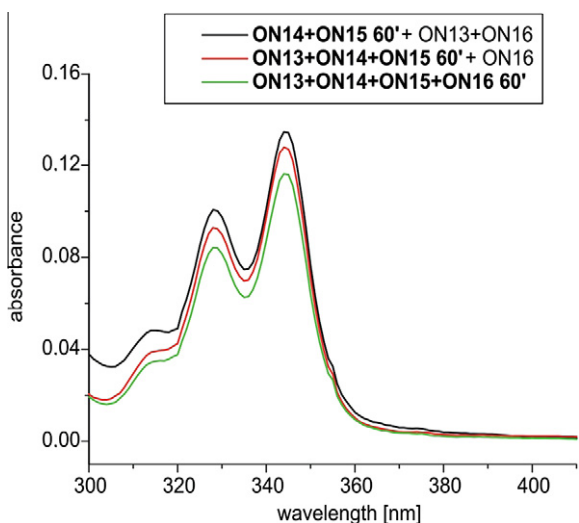


Figure 3. UV spectra comparison of order of photoligation of systems (ON14+ON15)60'+ON13+ON16 (black), (ON13+ON14+ON15)60'+ON16 (red) and (ON13+ON14+ON15+ON16)60' (green); UV induced photoadduct formation was performed after addition of two, three and four oligonucleotides, respectively, as indicated by underlining above, whereupon addition of the remaining strands (if relevant) was performed.

4.2. (1R,3R,4R,7S)-5-(Anthracen-9-ylmethyl)-1-(4,4'-dimethoxytrityloxymethyl)-7-hydroxy-3-(thymine-1-yl)-2-oxa-5-azabicyclo[2.2.1]heptane (2)

DMT protected 2'-amino-LNA nucleoside **1**³³ (200.0 mg, 0.35 mmol) was dissolved in anhydrous dichloroethane (4 ml) and 9-anthraldehyde (76.3 mg, 0.37 mmol) and sodium triacetoxyborohydride (111.0 mg, 0.52 mmol) were added. The mixture was stirred under an argon atmosphere at room temperature for 2 h. A saturated aqueous solution of sodium bicarbonate was added and the resulting mixture was extracted three times with dichloromethane. The combined organic phase was dried with anhydrous sodium sulphate, filtered and concentrated to dryness under reduced pressure to give a yellow foam. Purification of this residue by silica gel column chromatography (0–1% v/v MeOH/CH₂Cl₂) afforded nucleoside **2** (201.9 mg, 0.266 mmol, 76.0%) as a white foam. ¹H NMR (CDCl₃) δ 9.31 (1H, s, NH), 8.37–6.73 (23H, m, Ar),

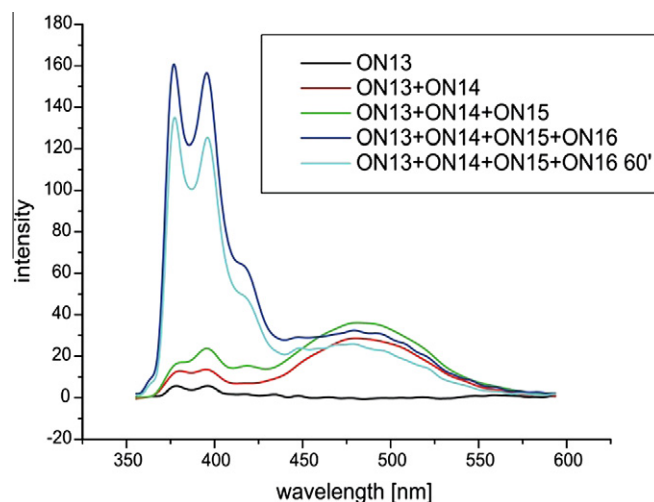


Figure 5. Fluorescence changes upon stepwise addition of branched oligonucleotides to form construct I. See text for explanation.

6.19 (1H, s, H1'), 5.24 (1H, s, 3'-OH), 5.16–4.91 (2H, m, Ar-CH₂), 4.26 (1H, d, *J* = 4.29, H-2'), 3.84 (1H, br s, H-3'), 3.71 (6H, s, 2 × OCH₃), 3.24–3.13 (2H, m, H-5'), 2.58–2.40 (2H, m, H-5''), 1.55 (3H, s, CH₃); ¹³C NMR (CDCl₃) δ 164.0, 158.5, 150.0, 144.4, 135.4, 135.3, 135.1, 131.3, 130.5, 130.0, 129.9, 129.2, 128.9, 127.9, 127.8, 126.9, 126.0, 124.8, 124.0, 113.1, 110.3, 88.7, 86.3, 82.8, 70.3, 67.2, 59.4, 55.1, 54.7, 45.4, 12.6; ESI-MS *m/z* 784.30 [M+Na]⁺ (calcd for C₄₇H₄₃N₃O₇, 784.30).

4.3. (1R,3R,4R,7S)-5-(Anthracen-9-ylmethyl)-7-(2-cyanoethoxy(diisopropylamino)phosphinoxy)-1-(4,4'-dimethoxytrityloxymethyl)-3-(thymine-1-yl)-2-oxa-5-azabicyclo[2.2.1] heptane (3)

To a solution of compound **2** (167 mg, 0.22 mmol) in anhydrous dichloromethane (4 ml) were added *N,N*-diisopropylammonium tetrazolidine (75 mg, 0.44 mmol) and 2-cyanoethyl-*N,N,N',N'*-tetraisopropylphosphoramidochloridite (153 μl, 80 mg, 0.48 mmol). The resulting mixture was stirred for 12 h at room temperature. A saturated aqueous solution of sodium bicarbonate was added and the resulting mixture was extracted three times with

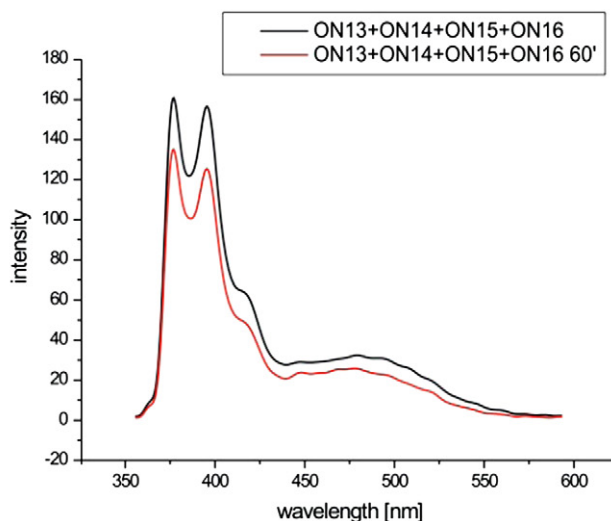
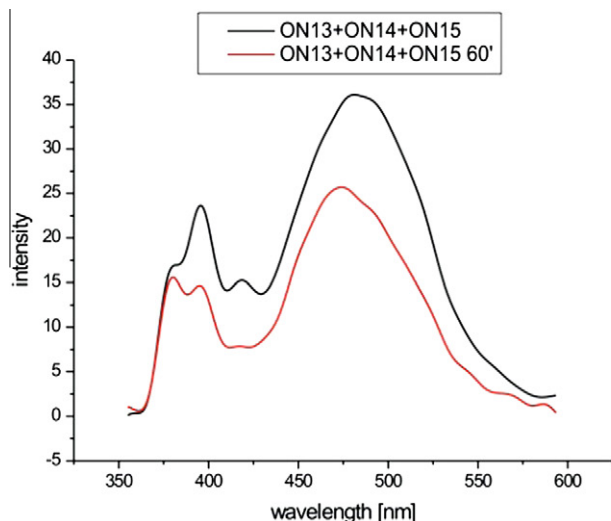


Figure 4. Fluorescence spectra before and after photoligation of systems ON13+ON14+ON15 (a) and ON14+ON15+ON13+ON16 (b).

dichloromethane containing 1% (v/v) of triethylamine. The organic phases were combined, dried with anhydrous sodium sulfate and concentrated to dryness under reduced pressure. The residue was purified by silica gel column chromatography using as eluent cyclohexane containing 1% (v/v) of triethylamine and a gradually increasing fraction of ethyl acetate (from 0% to 50%) furnishing product **3** as a white foam (144.4 mg, 68.5%). ^{31}P NMR (CDCl_3) δ 149.84 and 149.13. ESI-MS m/z : 984.41 $[\text{M}+\text{Na}]^+$ (calcd for $\text{C}_{56}\text{H}_{60}\text{N}_5\text{O}_8\text{P}$, 984.41).

4.4. Oligonucleotide synthesis

Modified oligonucleotides were synthesized using a standard DNA synthesis protocol with 15 min coupling time for the modified phosphoramidites **3** and **AD** (Schemes 1 and 2) and 30 minutes coupling times for the known phosphoramidites^{28,29} corresponding to 2'-amino-LNA monomers **T^{PyMe}** and **T^{PyCO}** (Scheme 2) on a Biosystems Expedite automated DNA synthesizer instrument in 0.2 μM scale. Coupling efficiencies varied from 70% in case of the **AD** amidite to 98% in case of 2'-*N*-amino-LNA derivatives. The procedure of asymmetric branching provided by the supplier (Glen Research) was used to enable synthesis of branched structures with the central **AD** monomer linking three different oligonucleotide strands. Cleavage of synthesized oligonucleotides from solid supports as well as removal of protecting groups was accomplished using standard conditions (32% aqueous ammonia, 55 °C, 12 h). Such DMT-ON prepared oligonucleotides were purified by RP-HPLC (Waters Prep LC 4000) followed by standard removal (80% AcOH, 20 min) of DMT protecting groups and precipitation (Acetone, -20 °C, 12 h). The composition of oligonucleotide products was verified by MALDI-TOF mass spectrometry and the concentrations were determined using a Beckman DU 800 spectrophotometer. The purity (>80%) of synthesized oligonucleotides was verified by ion-exchange HPLC (LaChrom L-7000 system equipped with a Dionex PA100 column using a gradient of 2–80% NaClO_4 in 0.2 M NaOH pH 12).

4.5. UV melting studies

Thermal denaturation studies involved duplex meltings in 1 mM phosphate buffer containing 1 M NaCl and 0.5 mM Na_2EDTA at pH 7.0. Such high ionic strength of the buffer was used in order to stabilize short, unligated oligonucleotides as well as it has been used in the literature.²² Oligonucleotide single strand concentrations were calculated from the absorbance above 80 °C and extinction coefficients were approximated by a nearest-neighbour model.^{38,39} Complementary oligonucleotides were mixed at a 1:1 ratio. Absorbance vs. temperature melting curves were measured at 260 nm with a heating rate of 1 °C/min from 5 to 95 °C on a Beckman DU 800 spectrophotometer equipped with a six-position microcell holder and thermoprogrammer. The measurements were taken for nine different concentrations of each duplex. Melting curves were analyzed and thermodynamic parameters calculated according to the two-state model with the program MeltWin 3.5. The majority of ΔH° values derived from T_M^{-1} versus $\ln(C_1/4)$ plots was within 15% of those derived from averaging the fits to individual melting curves (data not shown) as expected if a two-state model is valid.

4.6. Photoligation

Solutions of constructs (7.5 μM of each oligonucleotide) were prepared in 1 mM phosphate buffer containing 1 M NaCl and 0.5 mM Na_2EDTA , pH 7.0. Complementary strands were annealed for two minutes at 100 °C, whereupon the resulting mixture was slowly cooled to room temperature, cooled to 0 °C and irradiated

at 366 nm for 5, 10, 30, and 60 min using a high pressure mercury lamp (Philips, HPL, 125 W). The mixtures were analyzed by IC and UV-vis spectroscopy.

4.7. UV-vis spectra

7.5 μM solutions of each duplex were prepared and analyzed in 1 mM phosphate buffer containing 1 M NaCl, and 0.5 mM Na_2EDTA at pH 7.0. The spectra were recorded in the 200–500 nm wavelength range at 25 °C on a Beckman DU 800 spectrophotometer equipped with a six position microcell holder and thermoprogrammer.

4.8. Fluorescence steady-state emission spectra

Steady-state fluorescence emission spectra ($\lambda_{\text{em}} = 350\text{--}600$ nm) of given samples were recorded using Perkin Elmer LS 55 luminescence spectrometer with a temperature controller in 1 mM phosphate buffer containing 1 M NaCl and 0.5 mM Na_2EDTA , pH 7.0 using an excitation wavelength of $\lambda_{\text{ex}} = 350$ nm at 20 °C. For recording spectra 0.1 μM concentration of duplexes and 0.2–0.3 μM concentrations of the constructs involving branched constructs were used. Steady state fluorescence emission spectra were obtained as an average of five scans using an emission wavelength of 343 nm and a scan speed of 120 nm/min.

Acknowledgements

The Nucleic Acid Center is a research center of excellence funded by the Danish National Research Foundation for studies on nucleic acid chemical biology. We gratefully acknowledge financial support by The Danish National Research Foundation.

A. Supplementary data

Supplementary data associated with this article can be found, in the online version, at doi:10.1016/j.bmc.2011.10.052.

References and notes

- Rozkiewicz, D. I.; Gierlich, J.; Burley, G. A.; Gutsmedl, K.; Carell, T.; Ravoo, B. J.; Reinhoudt, D. N. *ChemBioChem* **2007**, *8*, 1997.
- Seeman, N. C. *Annu. Rev. Biophys. Biomol. Struct.* **1998**, *27*, 225.
- Xu, Y.; Kool, E. T. *J. Am. Chem. Soc.* **2000**, *122*, 9040.
- El-Sagheer, A. H.; Cheong, V. V.; Brown, T. *Org. Biomol. Chem.* **2011**, *9*, 232.
- Seo, T. S.; Bai, X.; Ruparel, H.; Li, Z.; Turro, N. J.; Ju, J. *Proc. Natl. Acad. Sci. U.S.A.* **2004**, *101*, 5488.
- El-Sagheer, A. H.; Kumar, R.; Findlow, S.; Werner, J. M.; Lane, A. N.; Brown, T. *ChemBioChem* **2008**, *9*, 50.
- Le Droumaguet, B.; Velonia, K. *Macromol. Rapid Commun.* **2008**, *29*, 1073.
- Moses, J. E.; Moorhouse, A. D. *Chem. Soc. Rev.* **2007**, *36*, 1249.
- Kolb, H. C.; Sharpless, K. B. *Drug Discovery Today* **2003**, *8*, 1128.
- Moran, N.; Bassani, D. M.; Desvergne, J.-P.; Keiper, S.; Lowden, P. A. S.; Vyle, J. S.; Tucker, J. H. *Chem. Commun.* **2006**, 5003.
- Kocalka, P.; El-Sagheer, A. H.; Brown, T. *ChemBioChem* **2008**, *9*, 1280.
- Ihara, T.; Mukae, M. *Anal. Sci.* **2007**, *23*, 625.
- Morvan, F.; Meyer, A.; Pourceau, G.; Vidal, S.; Chevolut, Y.; Souteyrand, E.; Vasseur, J.-J. *Nucleic Acids Symp. Ser. (Oxf)* **2008**, *52*, 47.
- Paredes, E.; Das, S. R. *ChemBioChem* **2011**, *12*, 125.
- Ihara, T.; Fujii, T.; Mukae, M.; Kitamura, Y.; Jyo, A. *J. Am. Chem. Soc.* **2004**, *126*, 8880.
- Ihara, T.; Mukae, M.; Tabara, M.; Kitamura, Y.; Jyo, A. *Nucleic Acids Symp. Ser. (Oxf)* **2005**, *49*, 41.
- Liu, J.; Taylor, J. S. *Nucleic Acids Res.* **1998**, *26*, 3300.
- Arslan, P.; Ihara, T.; Mukae, M.; Jyo, A. *Nucleic Acids Symp. Ser. (Oxf)* **2007**, *51*, 237.
- Fujimoto, K.; Yoshimura, Y.; Ikemoto, T.; Nakazawa, A.; Hayashi, M.; Saito, I. *Chem. Commun.* **2005**, 3177.
- Ami, T.; Fujimoto, K. *ChemBioChem* **2008**, *9*, 2071.
- Mukae, M.; Ihara, T.; Tabara, M.; Jyo, A. *Org. Biomol. Chem.* **2009**, *7*, 1349.
- Sinha, R. P.; Häder, D.-P. *Photochem. Photobiol. Sci.* **2002**, *1*, 225.
- Yamana, K.; Aota, R.; Nakano, H. *Tetrahedron Lett.* **1995**, *36*, 8427.
- Ranasinghe, R. T.; Brown, T. *Chem. Commun.* **2005**, 5487.
- Koch, T. J. *Phys.: Condens. Matter* **2003**, *15*, S1861.

26. Wengel, J. *Org. Biomol. Chem.* **2004**, *2*, 277.
27. Lindegaard, D.; Madsen, A. S.; Astakhova, I. V.; Malakhov, A. D.; Babu, B. R.; Korshun, V. A.; Wengel, J. *Bioorg. Med. Chem.* **2008**, *16*, 94.
28. Hrdlicka, P. J.; Babu, B. R.; Sørensen, M. D.; Harrit, N.; Wengel, J. *J. Am. Chem. Soc.* **2005**, *127*, 13293.
29. Hrdlicka, P. J.; Babu, B. R.; Sørensen, M. D.; Wengel, J. *Chem. Commun.* **2004**, 1478.
30. Højland, T.; Babu, B. R.; Bryld, T.; Wengel, J. *Nucleosides, Nucleotides Nucleic Acids* **2007**, *26*, 1411.
31. Babu, B. R.; Hrdlicka, P. J.; McKenzie, C. J.; Wengel, J. *Chem. Commun.* **2005**, 1705.
32. Umemoto, T.; Hrdlicka, P. J.; Babu, B. R.; Wengel, J. *ChemBioChem* **2007**, *8*, 2240.
33. Rosenbohm, C.; Christensen, S. M.; Sørensen, M. D.; Pedersen, D. S.; Larsen, L.-E.; Wengel, J.; Koch, T. *Org. Biomol. Chem.* **2003**, *1*, 655.
34. Abdel-Magid, A. F.; Carson, K. G.; Harris, B. D.; Maryanoff, C. A.; Shah, R. D. *J. Org. Chem.* **1996**, *61*, 3849.
35. Tucker, J. H. R.; Bouas-Laurent, H.; Marsau, P.; Riley, S. W.; Desvergne, J.-P. *Chem. Commun.* **1997**, *13*, 1165.
36. Greene, F. D.; Misrock, S. L.; Wolfe, J. R. *J. Am. Chem. Soc.* **1955**, *77*, 3852.
37. Bouas-Laurent, H.; Castellan, A.; Desvergne, J.-P.; Lapouyade, R. *Chem. Soc. Rev.* **2000**, *29*, 43.
38. Richards, E. G. In *Handbook of Biochemistry and Molecular Biology Nucleic Acids*; Fasman, G. D., Ed., third ed.; OH CRS Press: Cleveland, 1975; pp 596–603. Vol. 1.
39. Borer, P. N. In *Handbook of Biochemistry and Molecular Biology Nucleic Acids*; Fasman, G. D., Ed., third ed.; OH CRS Press: Cleveland, 1975; pp 589–595. Vol. 1.